COMPUTATIONAL PROBLEMS OF ELECTRICAL ENGINEERING

Vol. 13, No. 1, 2023

ELECTRON INTERACTION WITH POINT DEFECTS IN $CdSe_{0.35}Te_{0.65}$: JOINING OF AB INITIO APPROACH WITH SHORT-RANGE PRINCIPLE

Orest Malyk, Ihor Petrovych, Halyna Kenyo, Yurii Yurkevych, Yurii Vashkurak

Lviv Polytechnic National University, Lviv, Ukraine

orest.p.malyk@lpnu.ua, ihor.l.perovych@lpnu.ua, halyna.v.keno@lpnu.ua, yurii.s.yurkevych@lpnu.ua

https://doi.org/10.23939/jcpee2023.01.

Abstract: This study examines the problem of influence of point defects on transport phenomena in $CdSe_xTe_{1-x}$ (x=0.35) crystals. For the first time, the calculation of the electronic spectrum, wave function and potential energy of the electron in $CdSe_{0.35}Te_{0.65}$ samples at a prearranged temperature was carried out. Using the supercell method, the types of point defects were established, as well as the temperature dependence of their ionization energies in the studied temperature range. The temperature dependences of the deformation constants of the optical and acoustic scattering potentials were detected and also calculated the dependences on temperature of electron scattering constants on different crystal point defects. Temperature dependences of the mobility and Hall factor of electrons were found based on the scattering models on the short-range potential.

Key words: $CdSe_{0.35}Te_{0.65}$, transport phenomena, defects, ab initio calculation, short-range principle.

1. Introduction

$CdSe_xTe_{1-x}$ solid solution has a number of properties that are of interest for the production of electronic devices. This material exhibits photovoltaic properties sufficient for solar energy conversion, namely a large value of the absorption coefficient and the required band gap. Accordingly, researchers face the task of obtaining crystals of sufficiently high quality.

The optical and electrical properties of a semiconductor (in particular, the absorption coefficient and the transport phenomena) are highly dependent on the crystal lattice defects structure. The defects structure of the CdSeTe-based solar cell absorbing layer has been thoroughly investigated in references [1-12]. However, these works do not study the correlation between crystal lattice point defects and transport phenomena in the $CdSe_xTe_{1-x}$ solid solution. On the other hand, in reference [13] an attempt is made to establish such a relationship in solid solution $CdSe_xTe_{1-x}$ with sphalerite structure by applying two approaches: 1) using of the electron wave function and electron potential energy derived from first principles on the base of ABINIT program [14]; 2) application of the model of a charge carrier scattering on short-range potential of the different types of lattice point defects [15-19]. However, this work has a number of disadvantages: 1) the electronic wave function and electron potential energy used in this work correspond to the lowest state of the crystal (T=0) and therefore are unsuitable for describing the excited states of the crystal at T>0; 2) it is assumed that the structure of defects is limited to only one type of donor defect of unknown nature with ionization energy $\Delta E_D \approx 10$ meV, while the ionization energy of the defect is constant. In order to circumvent this difficulty, a method was developed for calculating the wave function of the electron and the potential energy of the electron in a solid solution CdSexTe1-x (x=0.35) with a sphalerite structure, which made it possible to describe the excited state of the crystal at T>0. Along with that, a method of determining the nature of donor point defects of various types was developed, which made it possible to estimate the ionization energy of these defects and its dependence on temperature. These approaches made it possible to consider transport phenomena in the $CdSe_{0.35}Te_{0.65}$ solid solution.

2. The method of calculating the wave function and self-consistent crystal potential at a given temperature

For the corresponding value of the composition of the solid solution, such a value of the lattice constant was chosen, which coincides with the experimental data. On the basis of this constant, the electronic wave functions and potential energies of the electron in CdTe and CdSe cells, as well as in Cd8Te8 and Cd8Se8 supercells were determined. All the calculations were performed using the ABINIT code [14].

For an ideal $CdSe_{0.35}Te_{0.65}$ solid solution, the electron wave functions and electron potential energies were determined as follows. At the first stage, calculations of the electronic function and potential energy of the electron were performed for ideal CdTe and CdSe cells (Cd atoms are located on the cell boundary, while Te (Se) atoms are located inside the cell). The method of selecting the GGA exchange-correlation potentials of Cd, Se, and Te, which served as output data, is presented in [20]. Next, a mixture of the Hartree-Fock exchange-correlation potential [21] and the above-mentioned exchange-correlation potentials was formed (this mixture is determined by the parameter α, which corresponds to the

«exchmix» parameter of the ABINIT code). The criterion for selecting the parameter α is as follows: at a prearranged temperature, the band gap theoretical value must cioncide with experimental value, which was obtained in reference [22, 23]:

$$E_{gCdSe} = 1.846 - 34.02\times 10^{-3}\left\{\left[1+(0.0119T)^{2.58}\right]^{0.388} - 1\right\} eV;$$

$$E_{gCdTe} = 1.65 - 5.35\times 10^{-4}\ T\ eV;$$

$$E_g(x,T) = x\,E_{gCdSe} + (1-x)E_{gCdTe} - 0.9\,x(1-x)\ eV.$$

Based on this approach, for a solid solution of a given composition, it is always possible to choose values A that correspond with the band gap at 0 K and 300 K. This method makes it possible to calculate the wave functions and potentials of ideal unit cells of CdTe and CdSe at 0 K and 300 K. The results of calculation are presented in Table I.

Table 1

Energy spectrum of CdTe and CdSe elementary cell

T=0, E_g=1.514 eV, Δ=1.526* eV		
Energy levels of CdTe elementary cell, eV	E_c- 1×(5.733) (0) E_v- 3×(4.219) (2)**	α=0.11387
Energy levels of CdSe elementary cell, eV	E_c- 1×(4.207) (0) E_v- 3×(2.693) (2)	α=1.20332
T=300 K, E_g=1.378 eV, Δ=1.483eV		
Energy levels of CdTe elementary cell, eV	E_c - 1×(5.674) (0) E_v- 3×(4.296) (2)	α=0.05202
Energy levels of CdSe elementary cell, eV	E_c- 1×(4.191) (0) E_v- 3×(2.813) (2)	α=1.1808

* Δ – a shift between the energy levels of ideal CdTe and CdSe elementary cells.

** Recording 3×(4.219) (2) means that there is exist 3-fold degenerate energy level with an occupation number equal 2.

From the Table 1 it follows that at a prearranged temperature the levels of E_c and E_v in the unit cells of CdTe and CdSe differ, which is caused by the presence of energy barriers between cells of different types. On the other hand, the experiment shows that at a predetermined temperature, the $CdSe_{0.35}Te_{0.65}$ solid solu-tion has the same bandgap width throughout the entire volume of the crystal. In our case, the discrepancy between theory and experiment can be circumvented as follows: we shift the energy levels of the CdSe cells up by the amount Δ, which is determined by the difference between levels of the bottom of the conduction band E_c (or the top of the valence band E_v) in the different neighboring elementary cells. As a result, a crystal with the same band gap width is obtained throughout the entire volume (see Fig. 1). An analogous result is obtained if the levels of the CdTe cell are shifted down by an amount Δ.

The following arguments are in favor of the proposed approach:

1. The bandgap width Eg represents the difference in levels, it is precisely this that is measured in the experiment, and not the values of the levels E_c and E_v. Accordingly, in each cell there is an arbitrary choice of the energy reference point.

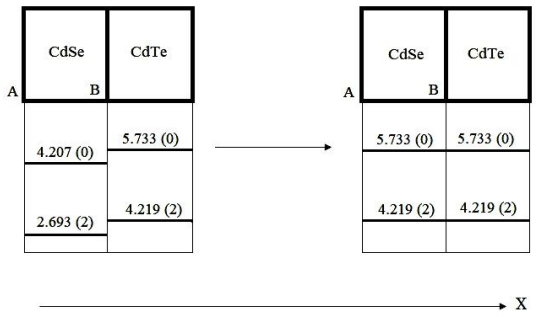

Fig. 1. The location along the X axis of ideal CdTe and CdSe elementary cells and the corresponding positions of the energy levels for ideal elementary cells at T=0 K for $CdSe_{0.35}Te_{0.65}$.

2. Cartesian coordinates in CdTe and CdSe cells are independent. Therefore, point A is the reference point of the coordinate system in the CdSe cell, point B is the reference point of the coordinate system in the CdTe cell.

The above method proposed for describing the ideal crystal of the $CdSe_{0.35}Te_{0.65}$ solid solution is similar (but not equivalent) to the method used in Riemann geometry. Namely, a three-dimensional manifold (in our case, a crystal) is described by a set of individual Cartesian coordinate systems used in a certain region of the manifold (in our case, CdTe and CdSe unit cells). That is, an ideal crystal of a solid solution is a set of CdTe and CdSe unit cells, for which the lattice constant and the theoretical value of the band gap coincide with the experiment.

Using the wave function and potential energy of the unit cell one can derived the wave function and derivatives of the potential energy over the coordinates of the cell atoms for the ideal $CdSe_xTe_{1-x}$ solid solution [13, 24]:

$$\left|\Psi(\boldsymbol{r})_{CdSeTe}\right|^2 = x\left|\Psi(\boldsymbol{r})_{CdSe}\right|^2 + (1-x)\left|\Psi(\boldsymbol{r})_{CdTe}\right|, \quad (1)$$

$$\partial U(\boldsymbol{r})_{CdSeTe}/\partial X_j = x\,\partial U(\boldsymbol{r})_{CdSe}/\partial X_j + (1-x)\partial U(\boldsymbol{r})_{CdTe}/\partial X_j, \quad (2)$$

$$\partial U(\boldsymbol{r})_{CdSeTe}/\partial Y_j = x\,\partial U(\boldsymbol{r})_{CdSe}/\partial Y_j + (1-x)\partial U(\boldsymbol{r})_{CdTe}/\partial Y_j, \quad (3)$$

$$\partial U(\boldsymbol{r})_{CdSeTe}/\partial Z_j = x\,\partial U(\boldsymbol{r})_{CdSe}/\partial Z_j + (1-x)\partial U(\boldsymbol{r})_{CdTe}/\partial Z_j, \quad (4)$$

where $j = 1,2$ is the numbering of the unit cell atoms. It should be noted that the derivatives in expressions (2)-(4) were calculated using the finite displacement method [18].

Using equations (1)-(4) and short-range scattering models [13, 15-19], it is possible to calculate the following electron scattering constants on crystal lattice defects, namely:

1. Scattering constants for an electron-polar optical phonon (PO), electron-piezoacoustic phonon (PAC) and electron-piezooptic phonon (POP) interaction

$$A_{PO} = A_{PAC} = A_{POP} = \int \left|\psi_{CdSeTe}\right|^2 (R^2 - r^2/3)\, d\boldsymbol{r}; \quad R = \sqrt{3}\, a_0/2 \qquad (5)$$

(a_0 – lattice constant). In (5) the region of integration includes two atoms of different sort and its volume is 1/8 of the volume of the unit cell of sphalerite.

2. d_0 – this value is equal to the largest value among the three values of the optical deformation potential (one longitudinal and two transverse branches of the optical vibrations of the crystal lattice). This constant describes an electron-nonpolar optical phonon (NPO) interaction:

$$d_{0\nu} = a_0 \int \left|\psi(\boldsymbol{r})_{CdSeTe}\right|^2 \varepsilon_\nu \cdot \boldsymbol{V}\, d\boldsymbol{r},\ \nu = 1,2,3 \qquad (6)$$

where the region of integration is 1/8 of the volume of the unit cell of sphalerite; $\boldsymbol{\varepsilon}_\nu$ – the unitary contravariant polarization vector of the optical oscillations. The components of the vector $\boldsymbol{V}$ are expressed through the corresponding linear combinations of derivatives (2)-(4), represented in the oblique coordinate system, formed by the primitive vectors of the sphalerite structure [24].

3. E_{AC} represents the acoustic deformation potential constant which is equal to the largest value among the three values of the acoustic deformation potential (one longitudinal and two transverse branches of the acoustic vibrations of the crystal lattice). This constant describes the electron-acoustic phonon interaction:

$$\begin{aligned} E_{AC||} &= (I_1/4 - I_2/2 - I_3/2); \\ E_{AC1\perp} &= (-I_1/2 + I_2/4 - I_3/2); \\ E_{AC2\perp} &= (-I_1/2 - I_2/2 + I_3/4); \end{aligned} \qquad (7)$$

$$I_1 = \int \left|\psi(\boldsymbol{r})_{CdSeTe}\right|^2 V_1'\, d\boldsymbol{r}';\ I_2 = \int \left|\psi(\boldsymbol{r})_{CdSeTe}\right|^2 V_2'\, d\boldsymbol{r}';$$

$I_3 = \int \left|\psi(\boldsymbol{r})_{CdSeTe}\right|^2 V_3'\, d\boldsymbol{r}'$; $V_1'; V_2'; V_3' 0$ are the compo-nents of the $\boldsymbol{V}$ vector similar to those in the case of NPO scattering.

4. The constant describing the electron scattering on the ionized impurity:

$$A_{II} = \int_\Omega \left|\psi(\boldsymbol{r})_{CdSeTe}\right|^2 \frac{1}{r}\, d\boldsymbol{r}, \qquad (8)$$

where integration is performed with respect to the unit cell volume of the sphalerite structure.

It should be noted that the integrals in expressions (5)-(8) were calculated using three-dimensional B-spline interpolation [25]. As it seen from (5)-(8), the scattering constants of the short-range models are equal to the integrals over the electron function $\psi(\boldsymbol{r})_{CdSeTe}$ and the potential $U(\boldsymbol{r})_{CdSeTe}$. Since the functions $\psi(\boldsymbol{r})_{CdSeTe}$ and $U(\boldsymbol{r})_{CdSeTe}$ at 0 K and 300 K differ, then, accordingly, the scattering constants are also different, that is, the temperature dependence of these parameters is observed. Based on these assumptions, it is possible to obtain linear dependences of scattering constants versus temperature:

$$\begin{aligned} A_{PO} &= \left(10.34 + 1.83 \times 10^{-4} T\right) \times 10^{-20}\, m^2; \\ d_0 &= -17.9 - -2.17 \times 10^{-3} T\, eV; \\ E_{AC} &= -2.12 - 2.5 \times 10^{-4} T\ eV; \\ A_{II} &= \left(0.496 - 3.33 \times 10^{-6} T\right) \times 10^{10}\, m^{-1}. \end{aligned}$$

The obtained temperature dependences of the scattering constants make it possible to calculate the electron scattering probabilities on different types of crystal defects [13] and, in turn, the transport properties of the solid solution $CdSe_{0.35}Te_{0.65}$.

3. Calculation of the temperature dependence of the ionization energy of crystal defects

The subject of research in this paper was such donor defects: Cd_{Te} , Cd_{Se} , V_{Se}–Cd_{Se}. The supercell method was used for the determination of the electronic spectrum ($1 \times 1 \times 2$ sphalerite cubic structure): for Cd_{Te} – supercell Cd_9Te_7; Cd_{Se} — supercell Cd_9Se_7; V_{Se}–Cd_{Se} – supercell Cd_9Se_6. At the same time, the electronic spectrum of ideal supercells was determined.

Spectrum calculations require determination of pseudopotentials. Pseudopotentials of Cd, Se, and Te atoms were created using the AtomPAW programs (Atompaw v3.0.1.9 and AtomPAW2Abinit v3.3.1) [26, 27]. The following valence basis states were used to construct the PAW functions: $5s^25p^04d^{10}$ for Cd, $4s^24p^4$ for Se and $4s^24p^65s^25p^4$ for Te. The values of the radii of the augmentation spheres are selected as follows: 2.2, 1.8 and 2.4 for Cd, Se and Te respectively. Within the density functional theory (DFT) (generalized gradient approximation (GGA) formalism proposed by Perdew, Burke and Ernzerhof (PBE) [20]) exchange and correlation effects were taken into account. To initialize the ABINIT program, the source files of the AtomPAW program containing the complete data set were used. The result of calculations of energy spectra of ideal supercells for the $CdSe_{0.35}Te_{0.65}$ solid solution is presented in Table II.

Data from Table II show the mismatch of spectral energy levels of ideal Cd_8Te_8 and Cd_8Se_8 supercells, which indicates the existence of energy barriers between Cd_8Te_8 and Cd_8Se_8 supercells. Therefore, as in the case of CdTe and CdSe unit cells, we shift the energy levels of the Cd_8Se_8 cells up by the amount Δ, which is deter-

mined by the difference between levels of the bottom of the conduction band E_c (or the top of the valence band E_v) in the different neighboring elementary cells. As a result, an ideal solid solution with the same band gap width is obtained throughout the entire volume, while the lattice constant also coincides with the expe-rimental value in the entire volume.

Table 1I

Energy spectrum of ideal Cd_8Te_8 and Cd_8Se_8 supercells.

T=0, E_g=1.514 eV, Δ=1.205 eV		
Energy levels of ideal Cd_8Te_8 supercell, eV	E_c- 1×(4.903) (0) E_v- 2×(3.389) (2)	α=-0.0676
Energy levels of ideal Cd_8Se_8 supercell,eV	E_c- 1×(3.698) (0) E_v- 2×(2.184) (2)	α=0.96685
T=300 K, E_g=1.378 eV, Δ=1.188 eV		
Energy levels of ideal Cd_8Te_8 supercell, eV	E_c- 1×(4.842) (0) E_v- 2×(3.464) (2)	α=-0.11244
Energy levels of ideal Cd_8Se_8 super-cell,eV	E_c- 1×(3.654) (0) E_v- 2×(2.276) (2)	α=0.82278

Table III compares the energy levels of ideal (the energy spectrum is shifted by a certain amount Δ) and defective (the energy spectrum is shifted by the same amount Δ) supercells. The data presented in Table III make it possible to calculate the activation (ionization) energies of various types of defects in the lattice of the CdSe0.35Te0.65 solid solution. Let us consider this using the example of Cd_{Te} and Cd_{Se} defects in $CdSe_xTe_{1-x}$ (x=0.35) at 0 K (see Fig. 2).

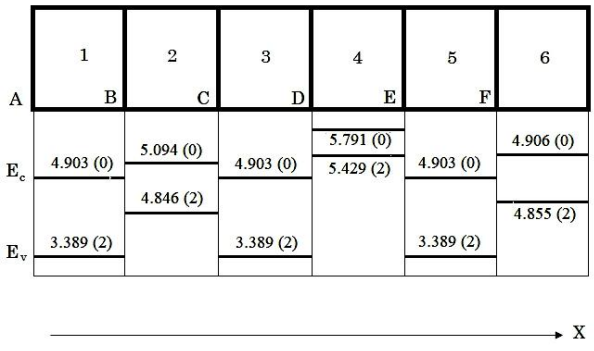

Fig. 2. The location along the X axis of ideal and defective supercells and the corresponding positions of the energy levels for ideal supercell, Cd_{Te} defect, Cd_{Se} defect and V_{Se}– Cd_{Se} defect at T=0 K for $CdSe_{0.35}Te_{0.65}$. 1,3,5 – ideal $Cd_8Te_8(Cd_8Se_8)$ supercell; 2 – defective Cd_9Te_7 supercell; 4 – defective Cd_9Se_7 supercell; 6 - defective Cd_9Se_6 supercell.

The idea of applying the supercell method to study the defect structure is as follows. Let's direct the X axis in the direction of the rib, the length of which is equal a_0, of the ideal or defective supercell. (see Fig. 2). Then the Y axis is directed along the rib of the supercell with the length a_0, and the Z axis is directed along the rib of the supercell with the length $2a_0$. Cd atoms are located at the nodes of the ideal (defective) supercell, located at the boundary of the supercell, and Te (or Se) atoms are located inside the ideal (defective) supercell. A lattice defect is always located inside a defective supercell.

Table 1II

Energy spectrum of ideal and defect supercell

T=0, E_g=1.514 eV		
Energy levels of ideal Cd_8Te_8 (Cd_8Se_8), eV	Energy levels of defect, eV	Ionization energy, eV
E_c- 1×(4.903) (0) E_v- 2×(3.389) (2)	Cd_{Te} 2×(5.094) (0) 1×(4.846) (2)	ΔE_D =0.057
E_c- 1×(4.903) (0) E_v- 2×(3.389) (2)	Cd_{Se} 2×(5.791) (0) 1×(5.429) (2)	ΔE_D =-0.526
E_c- 1×(4.903) (0) E_v- 2×(3.389) (2)	V_{Se}–Cd_{Se} 1×(4.906) (0) 1×(4.855) (2)	ΔE_D =0.048
T=300 K, E_g=1.378 eV		
E_c- 1×(4.842) (0) E_v- 2×(3.464) (2)	Cd_{Te} 2×(5.104) (0) 1×(4.861) (2)	ΔE_D =-0.019
E_c- 1×(4.842) (0) E_v- 2×(3.464) (2)	Cd_{Se} 2×(5.803) (0) 1×(5.436) (2)	ΔE_D =-0.594
E_c- 1×(4.842) (0) E_v- 2×(3.464) (2)	V_{Se}–Cd_{Se} 1×(4.915) (0) 1×(4.822) (2)	ΔE_D =0.020

For the Cd_{Te} defect, with the energy spectrum of the ideal Cd_8Te_8 (Cd_8Se_8) structure being compared with the energy spectrum of the defect (region 2) at T = 0 K, the transition of the electron from the defect level 1×(4.846) (2) to the conduction band level of the ideal structure 1×(4.903) (0) (with ionization energy ΔE_D = 0.057 eV) is seen to be most probable (see Fig. 2 and Table III). The remaining electronic transitions are unlikely due to very high ionization energy. At T = 300 K (see Table III), the electrons from the defect level 1×(4.861) (2) will pass to the level of the conduction band 1×(4.842) (0), i.e., the defect is completely ionized (ionization energy is less than zero and equal to ΔE_D =-0.019 eV).

Other electron transitions are unlikely due to high ionization energy. Assuming a linear temperature dependence of the defect ionization energy, this dependence can be determined.

For the Cd_{Se} defect, with the energy levels of the ideal structure being compared with the energy levels of the defect (region 4) at T=0 K, it is clear that all electrons from the defect level 1×(5.429) (2) will pass to the lower located level 1×(4.903) (0) of the conduction band (see Fig. 2 and Table III). This means that all Cd_{Se} defects at T=0 K will be ionized (ionization energy is nega-

tive ΔE_D = -0.526 eV). Analogous situation occurs at T=300 K., i.e., this type of defects in the range of 0÷300 K will be completely ionized. In a similar way, the temperature dependence of the ionization energies of the V_{Se}–Cd_{Se} defect can be calculated. As a result of the calculations, we will get:

$$Cd_{Te}\text{-}\Delta E_D = 0.057 - 2.54\times10^{-4}\,T;$$

$$V_{Se}\text{-}Cd_{Se} - \Delta E_D = 0.048 - 9.34\times10^{-5}\,T.$$

The method of describing the ideal and defective $CdSe_{0.35}Te_{0.65}$ crystal presented above is the result of a combination of the ab initio approach (calculation of the electronic spectrum of different regions of the crystal) and the short-range principle (energy (electron) transport occurs only between neighboring regions of the crystal).

4. Dicussion

The theoretical methods given in the two previous sections allow to study the kinetic properties of the $CdSe_xTe_{1-x}$ (x=0.35) solid solution in the temperature range of 10 – 400 K. Now let us make the following assumptions about the defects structure. Let the concentration of defects in the $CdSe_{0.35}Te_{0.65}$ solid solution be N_D (N_D=5×10^{14}÷5×10^{18} cm^{-3}). Then, the concentration of Cd_{Te} defects (these defects are formed in ideal Cd_8Te_8 supercells) is equal to

$$(1-x)N_D \Big/ \left\{1 + 2\,exp\left[\frac{F - \Delta E_{Cd_{Te}}}{k_B T}\right]\right\},$$

where F represents the Fermi level, and the reference point of the energy is at the bottom of the conduction band. Next, we assume that the concentrations of Cd_{Se} and V_{Se}–Cd_{Se} defects (these defects are formed in ideal Cd_8Se_8 supercells) are the same. That is, the total concentration of Cd_{Se} and V_{Se}–Cd_{Se} defects is equal to

$$\frac{xN_D}{2} + \frac{1}{2}xN_D \Big/ \left\{1 + 2\,exp\left[\frac{F - \Delta E_{V_{Se}-Cd_{Se}}}{k_B T}\right]\right\}.$$

Then, taking into account the transition temperatures of Cd_{Te} and V_{Se}–Cd_{Se} defects into the completely ionized state, we obtain an electroneutrality equation in the temperature range of 10÷400 K:

$$T < 224.9K;\; n - p = (1-x)N_D \Big/ \left\{1 + 2\,exp\left[\frac{F - \Delta E_{Cd_{Te}}}{k_B T}\right]\right\}$$

$$+ \frac{xN_D}{2} + \frac{1}{2}xN_D \Big/ \left\{1 + 2\,exp\left[\frac{F - \Delta E_{V_{Se}-Cd_{Se}}}{k_B T}\right]\right\};$$

$$224.9\,K < T : n - p = (1-x)N_D + \frac{1}{2}xN_D +$$

$$+ \frac{1}{2}xN_D \Big/ \left[1 + 2\,exp\left(\frac{F - E_{VseCdse}}{k_B T}\right)\right].$$

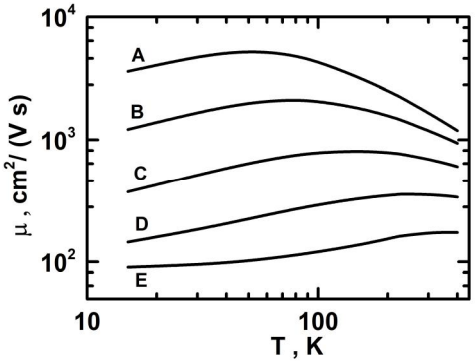

Fig. 3. Electron mobility versus temperature in $CdSe_{0.35}Te_{0.65}$ samples with a different defects concentration. A–N_D=1×10^{14} cm^{-3}, N_{SS}=1×10^{15} cm^{-3};B– N_D=1×10^{15} cm^{-3}, N_{SS}=3×10^{15} cm^{-3}; C– N_D=1×10^{16} cm^{-3}, N_{SS}=1×10^{16} cm^{-3}; D– N_D=1×10^{17} cm^{-3}, N_{SS}=3×10^{16} cm^{-3};E– N_D=1×10^{18} cm^{-3}, N_{SS}=8×10^{18} cm^{-3}.

Fig. 3 shows the calculated temperature dependences of electron mobility in samples with different concentrations of defects (donors and centers of static deformation (SS)). The electron mobility was calculated on the basis of short-range scattering models [13,15-19] using the exact solution of the Boltzmann kinetic equation [28]. In order to find out how well the approach proposed in this article adequately describes the physical reality, it is necessary to compare the theoretical $\mu(T)$ curves with experiment. However, as already pointed out by the author [13], there are practically no experimental data in the literature on transport phenomena in the $CdSe_xTe_{1-x}$ solid solution. The author knows only one literary source, which presents the study of electronic transport in this solid solution [29]. However, the investigated samples are polycrystalline (the grain size ~ 566÷755 Å). Accordingly, the experimental values of the electron mobility are anomalously small, which is due to the carriers scattering at the grain boundaries and indicates the low quality of the crystals.

Fig. 4a-4e reflect a comparison of different approaches (short-range and long-range scattering models) in the description of transport phenomena in $CdSe_{0.35}Te_{0.65}$ solid solution. Solid curves 1 obtained by the short-range electron scattering models and correspond to the exact solution of the Boltzmann kinetic equation. Dashed curves 2 and 3 obtained by the long-range electron scattering models (relaxation time approximation): curve 2 corresponds to the region of low temperatures $(\hbar\omega >> k_B T)$, curve 3 corresponds to the region of high temperatures $(\hbar\omega << k_B T)$.

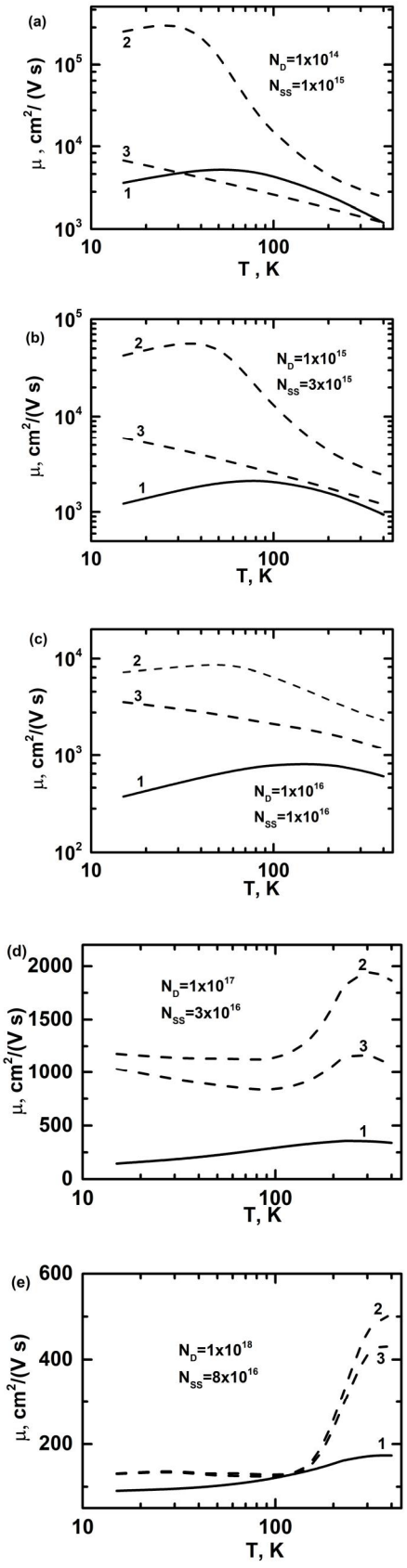

Fig. 4. Comparison of two theoretical approaches in $CdSe_{0.35}Te_{0.65}$ samples: 1– short-range scattering models; 2 and 3 – relaxation time approximation.

It can be seen from Figs. 4a-4e that these temperature dependences of electron mobility in the entire studied interval of temperatures and concentrations of defects are significantly qualitatively and quantitatively different from each other. The following observation should be made regarding the approach of relaxation time. It is known that for $CdSe_{0.35}Te_{0.65}$ the Debye temperature is equal to $\theta_D=258$ *K*. This means that the condition T <25.8 K limits the low-temperature region of this approximation, and the condition T >2580 K limits the high-temperature region of this approximation. It follows that the relaxation time approximation (corresponding to elastic scattering) is incorrect, because inelastic scattering takes place in the temperature interval 25.8 K< T <2580 K. On the other hand, the short-range scattering models make it possible to describe inelastic scattering. Thus, it can be argued that short-range models give a more adequate description of scattering processes in comparison with long-range models. Another confirmation in favour of the short-range scattering models are the curves presented in Fig. 4e. These curves are obtained by stitching the solutions of electroneutrality equations at the point of transition of one of the defects into a completely ionized state (at T=224.9 K). The temperature interval where the solutions are stitched is 1 K. Curves 1 demonstrate a fairly smooth transition in the stitching region, while curves 2 and 3 demonstrate a sharp (3.3–3.8 times) increase in mobility in the stitching region. However, there are no physical reasons for an increase in the electron concentration and conductivity in such a narrow temperature range. This indicates that curves 2 and 3 do not adequately describe the process of electron scattering on a crystal defect.

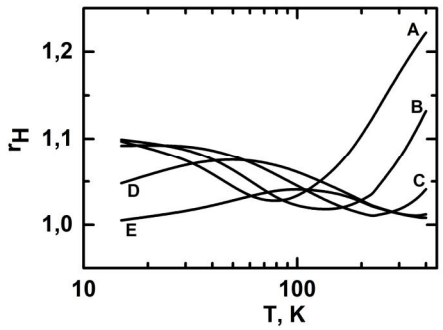

Fig. 5. Electron's Hall factor versus temperature in $CdSe_{0.35}Te_{0.65}$ samples with a different defects con-centration. The notation of the samples is the same as on Fig. 3.

The proposed method of calculation makes it possible to determine the dependence of the electron's Hall factor versus temperature for $CdSe_{0.35}Te_{0.65}$ (see. Fig. 5). As can be seen, at low temperatures in samples A, B, C (low defect concentration) and D the electron gas is non-degenerate or in an intermediate (between degenerate

and non-degenerate) state, while in sample E (high defect concentration) the electron gas is in a degenerate state. At high temperature region, the minima of the curves are existed in the region where the transition from the predominance of one scattering mechanism to another occurs. The higher defect concentration in the crystal correspnds the more higher temperature where the minimum of this dependence is existed.

Note that the presented calculation method was applied to a binary solid solution of $CdSe_xTe_{1-x}$ (sphalerite structure). In a similar manner, this calculation method can be used to another multicomponent solid solutions (sphalerite structure), in particular, to ternary, quaternary solid solutions. For example, for the binary solid solution $CdSe_xTe_{1-x}$, the supercell method was applied to two supercells Cd_8Te_8 and Cd_8Se_8, while for the description of the ternary solid solution CdSeSTe, one more supercell Cd_8S_8 must be added. In the future, it is necessary to apply the above-mentioned calculation method to three different types of supercells and determine the type of defects, as well as the temperature dependences of their ionization energies. By numerically solving the modified electroneutrality equation, the Fermi level is determined, which makes it possible to describe transport phenomena in the CdSeSTe solid solution. A similar approach can be applied to higher multicomponent solid solutions.

4. Conclusions

In the proposed article, for the first time, the calculation of the electronic spectrum, wave function and potential energy of the electron in $CdSe_{0.35}Te_{0.65}$ samples at a prearranged temperature was carried out. The proposed calculation method makes it possible to establish the dependence of electron scattering constants on various crystal defects versus temperature. This, in turn, made it possible to calculate the probability of electron scattering on crystal defects and, accordingly, to identify the kinetic coefficients of $CdSe_xTe_{1-x}$. Using the above-mentioned method for Cd_8Te_8 and Cd_8Se_8 supercells gave the opportunity to establish the structure of defects and to calculate the dependences of the ionization energies of point defects versus temperature. On the base of the short-range charge carrier interaction models with point defects determination the dependen-ces of electron mobility and electron's Hall factor versus temperature was done. The article also provides a comparison of the theoretical curves obtained by two competing approaches: a) short-range approach; b) long-range approach (relaxation time approximation). It was found that the kinetic properties of the $CdSe_xTe_{1-x}$ solid solution are more adequately reflected by the short-range scattering models. An example of using the proposed calculation method for a ternary solid solution is given. It is emphasized that this method can be used to describe the kinetic properties of higher multicomponent solid solutions with sphalerite structure.

References

[1] I. Sankin and D. Krasikov, "Kinetic simulations of Cu doping in chlorinated CdSeTe PV absorbers", *Phys. Status Solidi A*, vol. 215, p.1800887-1-11, 2019.

[2] J.H. Yang, et al., "First-principles study of roles of Cu and Cl in polycrystalline CdTe", *J. Appl. Phys.*, vol. 119, p. 045104-1-17, 2016.

[3] D. Krasikov, et al., "First-principles-based analysis of the influence of Cu on CdTe electronic properties", *Thin Solid Films*, vol. 535, pp. 322-325, 2013.

[4] Ji-Hui Yang, et al., "Review on first-principles study of defect properties of CdTe as a solar cell absorber", *Semicond. Sci.Technol.*, vol. 31 p. 083002-1-22, 2016.

[5] Ji-Hui Yang, et al., "Tuning the Fermi level beyond the equilibrium doping limit through quenching: The case of CdTe", *Phys. Rev. B*, vol. 90, p. 245202-1-5, 2014.

[6] V. Lordi, "Point defects in Cd(Zn)Te and TlBr: Theory", *J. Cryst. Growth*, vol. 379, p. 84-92, 2013.

[7] K. Biswas and M.H. Du, "What causes high resistivity in CdTe", *New J. Phys.*, vol. 14, p. 063020-1-20, 2012.

[8] I. Sankin and D. Krasikov, "Defect interactions and the role of complexes in CdTe solar cell absorber", *J. Mater. Chem. A*, vol. 5, pp. 3503-3515, 2017.

[9] A. Lindström et al., "High resistivity in undoped CdTe: carrier compensation of Te antisites and Cd vacancies", *J. Phys. D: Appl. Phys.*, vol. 49, p. 035101-1-12, 2016.

[10] A. Lindström, et al., "Cl-doping of Te-rich CdTe: Complex formation, self-compensation and self-purification from first principles", *AIP Adv.*, vol. 5, p. 087101-1 11, 2015.

[11] D.N. Krasikov, et al., "Theoretical analysis of non-radiative multiphonon recombination activity of intrinsic defects in CdTe", *J. Appl. Phys.*, vol. 119, p. 085706-1-10, 2016.

[12] J.H. Yang, et al., "Non-radiative carrier recombination enhanced by two-level process: a first-principles study", *Sci. Rep.*, vol. 6, p. 21712-1-10, 2016.

[13] O.P. Malyk, "Prediction of the kinetic properties of sphalerite $CdSe_xTe_{1-x}(0.1 \le x \le 0.5)$ solid solution: ab initio approach", *J. Electron. Mater.*, vol. 49, pp. 3080-3088, 2020.

[14] X. Gonze et al., "Recent developments in the ABINIT software package", *Comput. Phys. Commun.*, vol. 205, pp. 106-131, 2016.

[15] O.P. Malyk, "The local inelastic electron–polar optical phonon interaction in mercury telluride", *Comput. Mater. Sci.*, vol. 33, pp.153-156, 2005.

[16] O.P. Malyk, "Charge carrier scattering on the short-range potential of the crystal lattice defects in ZnCdTe, ZnHgSe and ZnHgTe", *Physica B: Condensed Matter*, vol. 404, 5022-5024, 2009.

[17] O.P. Malyk, "Electron scattering on the short-range potential of the crystallattice defects in ZnO", *Can. J. Phys.*, vol. 92, pp. 1372-1379, 2014.

[18] O. Malyk and S. Syrotyuk, "New scheme for calculating the kinetic coefficients in CdTe based on first-principle wave function", *Comput. Mater. Sci.*, vol. 139, pp. 387-394, 2017.

[19] O.P. Malyk and S.V. Syrotyuk, "The local electron in-teraction with point defects in sphalerite zinc selenide: calculation from the first principles", *J. Electron. Mater.*, vol. 47, pp. 4212-4218, 2018.

[20] J.P. Perdew, K. Burke, and M. Ernzerhof, "Generalized gradient approximation made simple", *Phys. Rev. Lett.*, vol. 77, pp. 3865-3868 (1996).

[21] P. Novák, et al, "Exact exchange for correlated electrons", *Phys. Status Solidi B*, vol. 243, pp. 563-572, 2006.

[22] G.L. Hansen, J.L. Schmit, and T.N. Casselman, "Energy gap versus alloy composition and temperature in $Hg_{1-x}Cd_xTe$", *J. Appl. Phys.*, vol. 53, pp. 7099-7101, 1982.

[23] R. Passler, "Parameter sets due to fittings of the temperature dependencies of fundamental bandgaps in semiconductors", *Phys. Status Solidi B*, vol. 216, pp. 975-1007, 1999.

[24] A. Haug, "Zur statischen Näherung des Festkörperproblems", *Z. Physik*, vol. 175, pp. 166-171, 1963.

[25] C. de Boor, *A Practical Guide to Splines*, New York: Springer-Verlag, 1978.

[26] N.A.W. Holzwarth, A.R. Tackett, and G.E. Matthews, "A Projector Augmented Wave (PAW) code for electronic structure calculations, Part I: atompaw for generating atom-centered functions", *Computer Phys. Comm.*, vol. 135, pp. 329-347, 2001.

[27] A.R. Tackett, N.A.W. Holzwarth, and G.E. Matthews, "A Projector Augmented Wave (PAW) code for electronic structure calculations, Part II: pwpaw for periodic solids in a plane wave basis", *Computer Phys. Comm.*, vol. 135, pp. 348-376, 2001.

[28] O.P. Malyk, "Nonelastic charge carrier scattering in mercury telluride", *J. Alloys Compd.*, vol. 371/1-2 pp. 146-149, 2004.

[29] N. Muthukumarasamy, et al., "Electrical conduction studies of hot wall deposited $CdSe_xTe_{1-x}$ thin films", *Sol. Energy Mater. Sol. Cells* , vol. 92, pp. 851-856, 2008.

РУХЛИВІСТЬ ЕЛЕКТРОНІВ У $CdSe_{0.35}Te_{0.65}$: ПОЄДНАННЯ Ab Initio ПІДХОДУ З ПРИНЦИПОМ БЛИЗЬКОДІЇ

Орест Малик, Ігор Петрович,
Галина Кеньо, Юрій Юркевич,
Юрій Вашкурак

У даній роботі розглядається проблема впливу точкових дефектів на явища переносу в кристалах $CdSe_xTe_{1-x}$ (x=0,35). Вперше проведено розрахунок електронного спектру, хвильової функції та потенціальної енергії електрона в зразках $CdSe_{0.35}Te_{0.65}$ при заданій температурі. За допомогою методу суперкомірки встановлено типи точкових дефектів, а також температурну залежність їх енергій іонізації в досліджуваному інтервалі температур. Виявлено температурні залежності констант деформації оптичного та акустичного потенціалів розсіяння, а також розраховано температурні залежності констант розсіяння електронів на різних кристалічних точкових дефектах. На основі моделей розсіювання на короткодіючому потенціалі знайдено температурні залежності рухливості та холлівського фактора електронів.

Orest Malyk was born on Nov, 12, 4 960,62 cm Lviv, Ukraine. His current position is a professor of the Semiconductor Electronics Department at Lviv Polytechnic National University (Lviv, Ukraine). O. Malyk has been Doctor of Phys.-Math. Sciences (speciality 01.04.10 – Physics of Semiconductors and Dielectrics) since 2018. He is the author and co-author of more than 160 scientific papers. His scientific interests include transport phenomena in compound semiconductors, charge carrier scattering on the crystal defects within the framework of short-range scattering models, calculation of kinetic properties of semiconductors on the basis of ab initio approach.

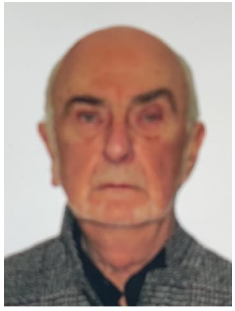

Ihor Petrovych was born on Jan, 18, 1945 in Lviv, Ukraine. His current position is an associate-professor Docent of the Department of Physics at Lviv Polytechnic National University (Lviv, Ukraine). I.Petrovych has been Ph. D of Phys.-Math. Sciences (speciality 01.04.07. – Solid States Physics) since 1982. He is the author and co-author of about 60 scientific papers. His scientific interests include experimental investigations of optical properties of compound semiconductors, calculation kinetic properties of small-gaps semiconductors.

Halyna Kenyo was born in 1961. She received a degree in semiconductor and microelectronic devices (electronic engineer) and Ph. D degree in solid state electronics including functional from Lviv Polytechnic National University, Lviv, Ukraine, in 1983 and 1995, respectively.

She is currently employed as an associate-professor at the Department of Information Security, Lviv Polytechnic National University. She is the author and co-author of about 30 scientific papers. Her scientific interests include: transport phenomena in compound semiconductors, physical and technical modelling of acoustic processes, Internet of things security.

Yurii Yurkevych was born on June, 21, 1959 in Lviv, Ukraine. His current position is an associate-professor Docent of the Department of Heat and Gas Supply and Ventilation at Lviv Polytechnic National University (Lviv, Ukraine). Y. Yurkevych has been Candidate of Technical Sciences (speciality 05.23.03 – Ventilation, Lighting and Heat and Gas Supply) since 1997. He is the author and co-author of more than 50 scientific papers and 9 author's certificates of patents of Ukraine. The field of his scientific research: increasing the efficiency of fuel use in heating, gas supply and ventilation systems.

Yuri Vashkurak was born on April 14, 1958 in Lubny, Poltava region. His position is an associate professor of the Department of Automation and Computer-Integrated Technologies at Lviv Polytechnic National University (Lviv, Ukraine). Y. Vashkurak has been candidate of technical sciences (speciality 05.11.13 – devices and methods of control and determination of the composition of substances) since 1988. He is author and co-author of about 100 scientific papers. The range of scientific interests includes transport phenomena in complex environments, determination of the value of charge carrier's scattering.

Received: 17.04.2023. Accepted: 18.06.2023